Mechanics & Industry **20**, 812 (2019)
© AFM, EDP Sciences 2020
https://doi.org/10.1051/meca/2020056

Mechanics & Industry

Available online at:
www.mechanics-industry.org

Selected scientific topics in recent applied engineering – 20 Years of the 'French Association of Mechanics – AFM'

Regular Article

Proof of a composite repair concept for aeronautical structures: a simplified method

Francis Collombet[1,*], Yves Davila[1], Sergio Avila[2], Alexander Morales[2], Laurent Crouzeix[1], Yves-Henri Grunevald[3], Hilario Hernandez[2], Nathalie Rocher[1], and François Cénac[4]

[1] Université de Toulouse, UPS, INSA, Mines d'Albi, ISAE, ICA (Institut Clément Ader). Espace Clément Ader, 3 rue Caroline Aigle,31400 Toulouse, France
[2] Instituto Politecnico Nacional, ESIME Ticoman. Av. Ticoman N° 600, 07340 Ciudad de Mexico, Mexico
[3] Composites, Expertise & Solutions. 131 Traverse de La Penne aux Camoins, 13821 La Penne-Sur-Huveaune, France
[4] Bayab Industries, 10 allée de Longueterre, 31850 Montrabé, France

Received: 7 October 2019 / Accepted: 16 June 2020

Abstract. This paper provides an illustration of all stages of primary aeronautical composite structure repair by using industrial tools and scientific methodologies, as well as numerical tools to simplify the cross-over analysis of the mechanical behaviour of the repaired area. Economically and scientifically speaking, one of the main challenges of composite repair (for monolithic long fiber composite parts) consists of promoting a bonded composite patch option without additional riveted doublers. To address this challenge, size reduction of the patch could be mandatory. A patent (jointly owned by ICA, Bayab Industries and CES), entitled "Method for repairing a wall consisting of a plurality of layers", is devoted to reducing repair patch dimensions of monolithic composite parts provided the bonding zone has a stepped-lap geometry. This patent is based on a simple idea that no overlapping length is required between composite plies for load transfer except in the fiber directions of the plies (unidirectional or biaxial long fiber reinforcements with epoxy matrix). To prove this concept, we consider on one hand, a situation unusual in the literature by studying a composite specimen without fibers aligned along the main loading axis, and on the other hand, a classical situation of where the shape of the specimen is adapted to be studied by uniaxial tension tests. After different manufacturing steps, the studied specimen contains three zones representing both the influence of the total thickness of a repair patch, the stepped-lap area assembled with an adhesive film and the parent composite part. Basically, a simple parent structure consisting of 16 plies of UD Hexply® M21/35%/268/T700GC (close to Airbus composite raw materials on board in A380) is manufactured with a stacking sequence of $[+45/-45/-45/+45/+45/-45/-45/+45]_s$. Then, the parent structure is machined by the Airbus Abrasive Water Jet machine and the final repair area has a stepped-lap geometry by overlapping successive plies of the same nature as the parent plate and after having previously applied an adhesive film (cured at 180 °C). Furthermore, 3 values of overlap length (respectively, 6, 8 and 13 mm) are investigated to include the mean value required by Airbus in the case of the use of the studied prepreg. After abrasive water jet machining of the composite parent part, repair patch manufacturing was performed according to Airbus requirements. The studied specimens were cut from the final plate (involving the parent plate, the stepped lap zone and the zone of the patch itself) and tested in an uniaxial tensile configuration with a loading direction shifted 45° with respect to the fiber direction. Furthermore, studying uniaxial tensile tests on multilayer-pasted interface is innovative in the literature. In this paper, it is shown that the stepped-lap area assembled with an adhesive film is not the weak link of the mechanical response but rather the parent area, i.e. the unrepaired monolithic composite. Numerical calculations confirm this proof of concept by underlying that the level of shear stress in the adhesive film, for these three overlapping values, is below the chosen limit value. These results show that the patch size reduction is possible.

Keywords: Composite repair / abrasive water jet machining / composite bonded assembly / light finite elements modelling / mechanical testing

* e-mail: francis.collombet@iut-tlse3.fr

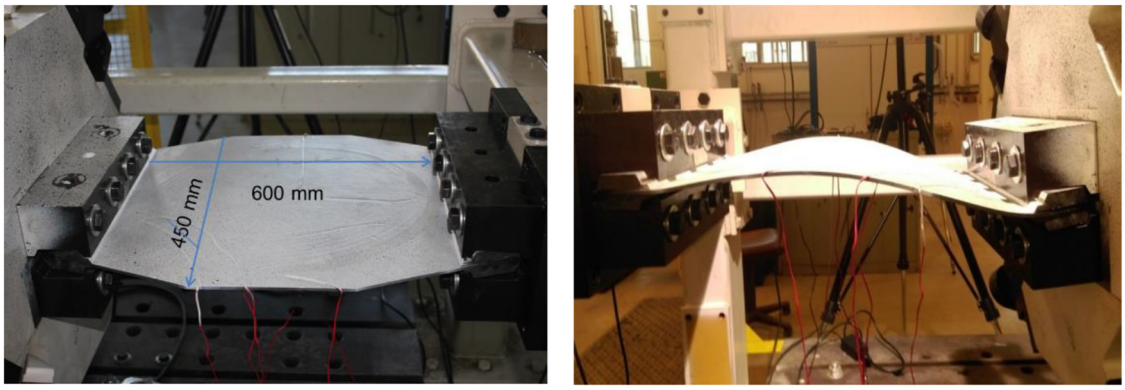

Fig. 1. View of the repair evaluator with (a) the start and (b) the last phase of the multiaxial mechanical test, see [5] for details.

1 Introduction

This paper deals with scientific and technical issues related to the repair of aeronautical structures, made of multilayer monolithic long fibre composites. There is an increasing need for such repairs due to the entry into service of hundreds of B787 and A350 aircraft per year. In the repair process, according to the customer services of the aircraft manufacturers, one of the issues is to limit the influence of the area and/or the volume of removal of material and reduce the prohibitive time of immobilization of the aircraft (which costs the operating company roughly 100–200 kUS dollars per day).

According to this Specification of Work (SoW), a joint patent [1] held by the Clement Ader Institute, the two SMEs Composites Expertise & Solutions and Bayab Industries, is of interest because it is based on a simple idea that a nominal overlapping length is only necessary in the direction of each UD ply. This patent allows the description and modelling of a minimum volume of material to be removed while ensuring a nominal transfer of efficient stress flow between the parent composite part and the repair patch. To give some orders of magnitude, it was shown that this approach can lead to the reduction of the repair patch grip by more than 70% [2], making the adhesive patch certifiable by aeronautic regulation authorities [3]. Actually today, the bonding repair patch is allowed alone (i.e. without additional riveted doublers [4]) only if its loss is not an impediment to the limit loading transfer ("patch-off" concept). In aeronautics [3], all critical structures will have a repair size limit no larger than a size that allows Limit Load strength to be achieved with the repair failed or failed within constraints of the arresting design features (in the repair or base structure). This approach is needed to ensure Limit Load capability in the event of bonded repair failures.

Two geometries for bonding composite repair patch are used in aeronautic industry with respectively tapered scarf and stepped-lap joints. During thirty years, Boeing employed only scarf geometry to repair composite primary aeronautic structures. Airbus was the first to introduce the stepped-lap geometry for composite repair. As regards the overlapping length, Airbus was more conservative than Boeing. For example, Airbus requires 8 mm overlap for 0.13 mm ply thickness while Boeing 5 mm overlap for the same ply thickness. We have chosen stepped-lap geometry for taking the best performance in terms of patch size reduction [2].

To be close to industrial applications, an original methodology of mechanical characterization (called Multi-Instrumented Technological Evaluator tool box) has been proposed [2,5]. The MITE tool box allows the design of case-by-case specific repair evaluators that can be tested in a multi-axial testing machine under complex loading sequences. For achieving such approach, metric composite parts are mandatory according to the real patch repair size and the definition of the SoW because of the case-by-case nature of the composite repair issues. The proof of the interest of the joint patent has been done in the past thanks to the Multi-Instrumented Technological Evaluator tool box [5], cf. Figure 1.

The originality of the current paper lies in the choice of a composite specimen (i.e. a composite part with a simpler geometry compared to a composite repair evaluator but in the framework of an unusual situation because this specimen will be tested without fiber directions in the main loading axis using a classical tension set-up (cf. Fig. 2). Furthermore, whatever the chosen stacking sequence, studying uniaxial traction tests on multilayer-stepped interface is innovative in the literature.

On Figure 2, only the half thickness is shown for clarity. On Figure 2a, the stacking sequence is quasi-isotropic and frequent in the world of composites and in aeronautics. The performance of our approach for such a stacking sequence has been demonstrated on the technological evaluator, and works. Most of the loading flow goes through the plies at 0° and therefore the associated bonded assemblies. The ruptures of the part and the bond occur at the same time (because of the plies at 0°). It is therefore difficult to know if the bond has been damaged due to the part rupture or vice versa. Furthermore, a tension set-up with an adequate loading capacity is not easily available for such stacking sequences. On Figure 2b, an unusual stacking sequence is shown, only used for demonstration. It has no industrial utility, except for a torsion shaft, but

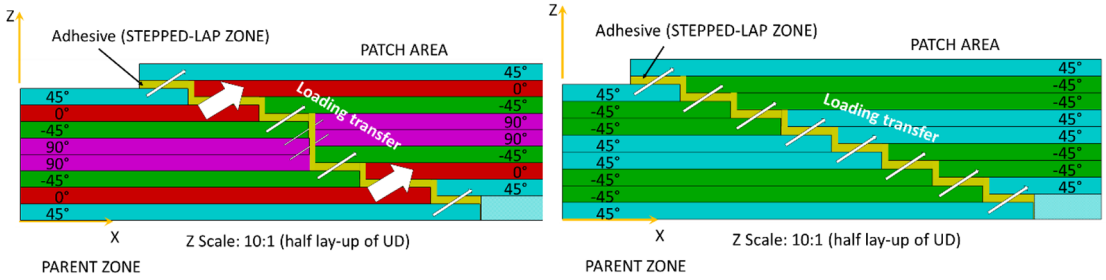

Fig. 2. Illustration of two situations of composite specimens with stepped lap respectively with, (a) classical stacking sequence and (b) unusual stacking sequence (scheme of loading transfer and its intensity under tension indicated by the white arrows with respect to their size and direction).

it allows verification that the bonded area is not the weak link in the system using a classical tension set-up.

To illustrate our purpose, we have chosen to study a parent plate consisting of 16 plies of UD Hexply® M21/35%/268/T700GC prepreg cured in autoclave at 180 °C, for this first stage, with a stacking sequence: [+45°/−45°/−45°/+45°/+45°/−45°/−45°/+45°/+45°/−45°/−45°/+45°/+45°/−45°/−45°/+45°/+45°/ −45°/−45°/+45°] i.e. $[((+45°/-45°)_s)_s]_s$.

The second stage of this study corresponds to a machining phase using an abrasive water jet technique for the composite milling. This phase was performed with the mobile machine called REPLY.5, designed by the innovative small company Bayab Industries. It is the only machine certified by Airbus to repair primary structures on the A350 [6].

The third phase concerns the lay-up of the stepped-lap with the same material after having previously stacked an adhesive film. The total length of the UD is sufficient to provide a final plate with the composite bonding assembly zone located far away from its extremities (grip zones during the test). The fourth phase is devoted to the polymerization of the adhesive film and the added composite plies. The patch zone and the added monolithic zone polymerization is performed using the portable hot bonder Aeroform AHB-380, to be in accordance with the in situ Airbus repair requirements [6]. Different overlap lengths (6, 8 and 13 mm) are considered to surround the overlapping value recommended in aeronautics by providing a step ratio of about 1/30. Indeed, the overlapping distance is expressed as a ratio of the ply thickness, and, in aeronautical applications, this ratio is usually 30 (which is roughly the ratio between 8 mm overlap length and 0.26 mm ply thickness), whatever the fibre orientation with respect to the main loading direction.

The fourth phase is devoted to cut test coupons from parent plates with these three overlap ratios, 20, 30 and 50 respectively, to perform uniaxial tests. As was explained previously, this situation is unusual but represents a good comprise between a simple manner to test (uniaxial tension) and the material orientation to study if a nominal overlap length is strictly necessary in the direction of the UD fibres.

In a fifth phase, a finite element study was performed in parallel with the experimental investigation. The repair zone was modelled through an innovative multi-scale method [7] in which the composite substrates are modelled through shell elements and the adhesive joint consists of volume elements. The aim is to avoid the use of overly heavy finite element calculations such as described in [8], as this penalizes the design of large repaired structures, making cross-test calculations very time-consuming. The numerical model shows that the non-repair zone is the weak link of these coupons and not the overlapped region. These numerical results confirm the experimental observations during tension tests.

2 Manufacturing and abrasive water jet machining process

The first stage of this study corresponds to the fabrication and machining process of a monolithic carbon-epoxy composite plate. For this study a 16 ply composite plate of $[((+45°/-45°)_s)_s]_s$ was made from a UD Hexply® M21/35%/268/T700GC prepreg, cured in autoclave at 180 °C. Afterwards the plate is cured and then machined. Three step ratios (step length over ply thickness) were studied, 20, 30 and 50, which roughly correspond to overlap lengths of 6 mm, 8 mm and 13 mm respectively. The machining is done using the abrasive water jet (AWJ) removal technique. The AWJ blind machining was performed by a mobile machine (REPLY.5, cf. Fig. 3).

AWJ is the only technique allowing an offset machining "layer by layer" of multi-layered composite material (to be capable to take into account the variability of the composite part [9]). This is very difficult with the cutting tools used by the conventional techniques [10].

The REPLY.5 AWJ machine consists of three principal elements, the control unit which contains the pump and the control system (cf. Fig. 3a), the abrasive water jet equipment (which is light −50 kg − compared to the competing project attempts) and the control panel to operate the machine (cf. Fig. 3b).

After fixing the composite plate onto the workbench, the AWJ machine is placed on top of it and is maintained in position with suction cups (cf. Fig. 4a). In an industrial situation, this suction system allows the positioning of the machine onto a composite fuselage. The machine is then levelled to roughly adjust the distance between the AWJ head (nozzle) and the composite part (cf. Fig. 4b).

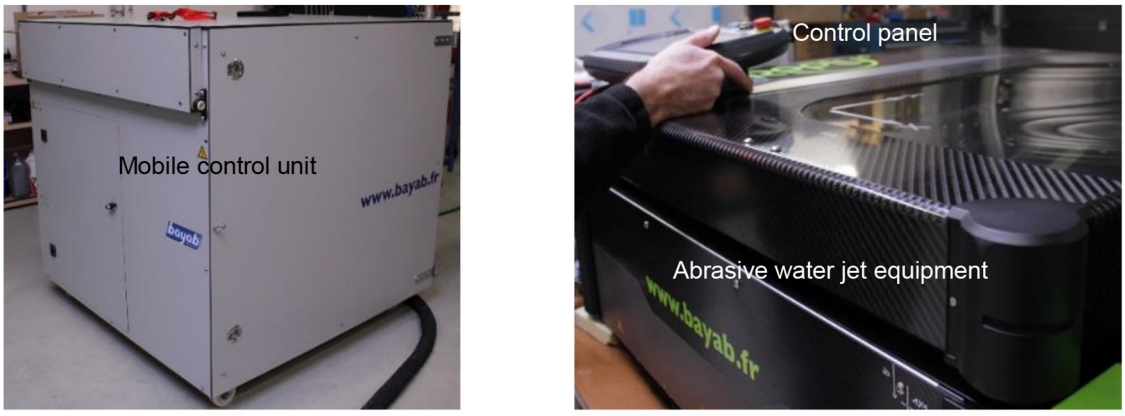

a) **b)**

Fig. 3. Bayab Industries abrasive water jet machine REPLY.5 with (a) control unit and (b) abrasive water jet equipment (50 kg) and control panel.

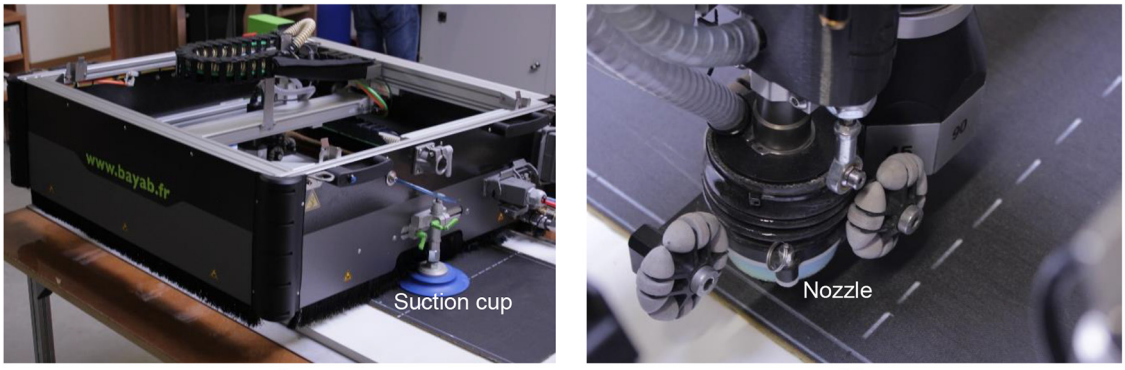

a) **b)**

Fig. 4. Abrasive water jet machine Reply.5 with (a) levelled machine and (b) nozzle.

The waste generated during the machining process (composed by composite dust, abrasive particles and water) is removed by a patented aspirator system.

The machine is aligned by a laser level to the marked along the x- and y-main directions of the studied parent composite plate (cf. Fig. 5).

After aligning the machine, the layer of composite material corresponding to the first step (here ply #16) is removed. As an illustration, the first machined step for the step lap ratio of 20 is presented in Figure 6. For the other step lap ratios of 30 and 50, the same procedure is applied. The cut trajectory and cut parameters (water jet pressure, and nozzle feed rate) are programmed into the machine. These parameters are Intellectual Property of Airbus and Bayab Industries and have not been disclosed.

Once the machining process in one ply is finished, a verification is done by means of image analysis using the camera installed on the AWJ machine and a lighting of the machined zone through a set of four low-angled lights aimed in the four possible orientations of the reinforcement respectively, 0°, 90°, +45° and −45° (cf. Fig. 7a). To verify the fibre direction of the ply below, the camera takes four different images using each lighting angle. Indeed, the lightning emitted by the low-angled light is diffracted differently depending on the angle with respect to the long fibre orientation. The control unit compares the recorded images pixel-by-pixel. For accurate information, a selection of images from the screen of the control panel (cf. Fig. 7b)

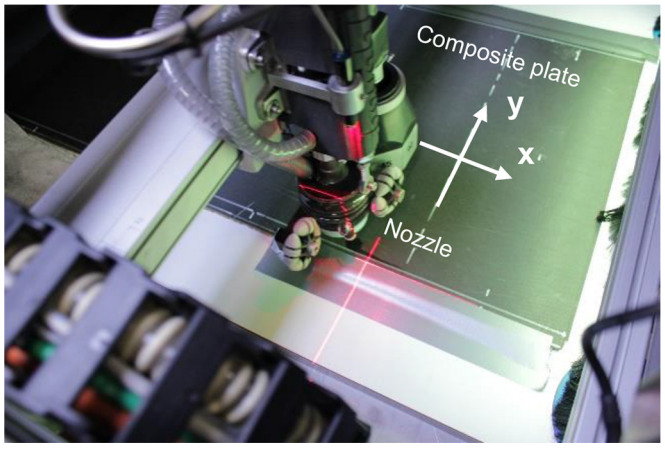

Fig. 5. Alignment process of the nozzle over the x- and y-main directions of the composite plate.

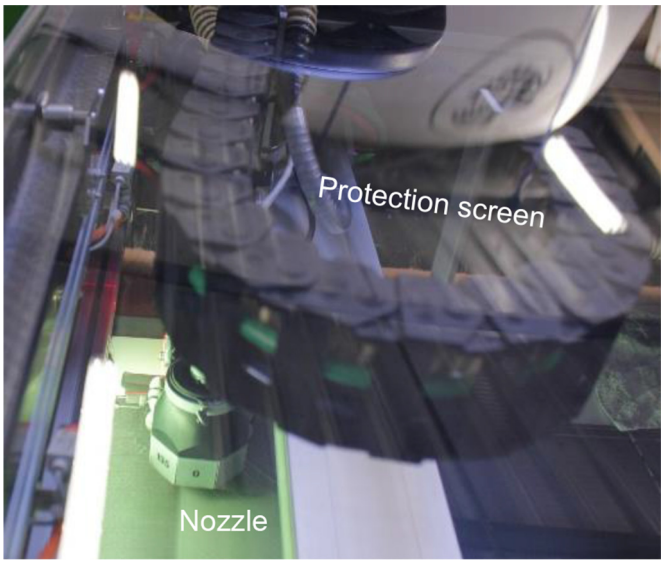

Fig. 6. View through the protection screen of the machine during the machining of the step #1 for the stepped lap ratio of 1:20 (step length over ply thickness).

shows an estimation of the matrix ratio (percentage of dark spots thanks to no light diffraction, ≈60% according to ply thickness variabilities, [9]) in an interface between two plies. The matrix ratio is evaluated to ensure that just one ply was removed. This is an alternative to direct measurement of the cut depth.

Afterward, the process or nozzle alignment, machining and verification are repeated. As an illustration, the resulting stepped lap profile (step ratio of 20) is shown in Figure 8.

3 Repair process

After completion of the machining process, the composite plates are cut in halves in order to create the possibility of repairing two sets of plates for each overlap ratio (cf. Fig. 8). This situation is representative of a "through hole" repair. We label the parent plate as "Plate 13", corresponding to a step length of 13 mm or a step ratio of 50, as shown in Figure 9 and hereafter as an illustration in this paper. Typical Airbus repairs require that the material of the repair patch should be cured at 120 °C, in order to not

a) **b)**

Fig. 7. Verification process of the machining surface with (a) overlap zone analysed by image analysis and (b) visualization and selection of the images on the control panel to estimate the location of the interface between to plies (i.e. presence of numerous dark spots due to no light diffraction).

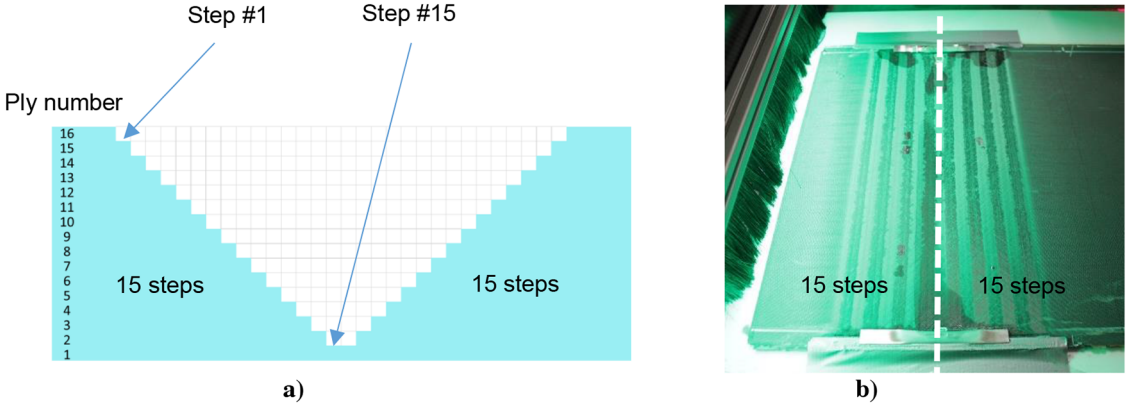

a) **b)**

Fig. 8. Machining of the 15 steps (for 16 plies in total) with (a) scheme of milled profile (not to scale) and (b) view of the finished milled stepped-lap for the overlap ratio of 20.

thermally degrade the material of the parent structure, which was cured at 180 °C, if applying a certain number of cure cycles of the repair patch. However, in the repairs presented here, in order to limit the influence of the different materials in the final tested structure, the chosen repair material of the reconstituted zone is the same one as that of the parent plate, i.e. Hexply® M21/35%/268/T700GC and the adhesive film was cured at 180 °C as well. However, to be close to the Airbus repair process requirements, the curing process for the parent plate is performed with a portable hot bonder machine under only vacuum instead of being placed in an autoclave [6].

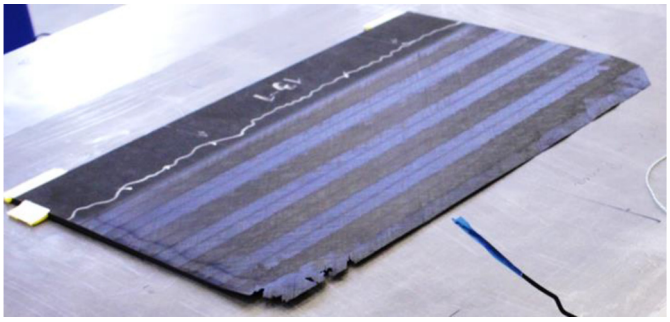

Fig. 9. View of parent composite plate noted "Plate 13" (overlap length of 13 mm), shown after AWJ milling phase and before the repair patch installation.

An adhesive film of Hexcel Composites Hexbond® is placed between the repair plies and the parent plate to assure that the surface of the parent structures (already cured) adheres completely to the repair patch (to be cured). This film is cured at 180 °C, to be compatible with the cure cycle of M21 resin of the repair plies.

The surface of the stepped-lap area is degreased and cleaned using alcohol and/or acetone. The repair procedure is composed of different phases. First, the adhesive film of Hexbond® is placed in the stepped-lap area (cf. Fig. 10a). Then, the repair plies are stacked, for the first ply (cf. Fig. 10b) to the sixteenth repair ply (cf. Fig. 10c), using guidelines drawn on the surface of the tooling for adequate ply placement (cf. Figs. 10b and 10c). In the industry (aircraft repair and maintenance), guidelines painted onto the surface of the parent structure (like the aircraft fuselage) are indeed used not only for ply placement but also for ply orientation purposes. After the repair is done, the repaired surface will be cleaned and painted as per SRM indications (Structural Repair Manual [6]).

Once all the repair plies are laid up, the vacuum bag is installed. The sequence of vacuum bag materials is done as per Airbus SRM indications for structural composite repair (cf. Fig. 11).

Once the vacuum bag is placed and sealed, a vacuum test is performed. The vacuum is applied using the external vacuum pump (cf. Fig. 12).

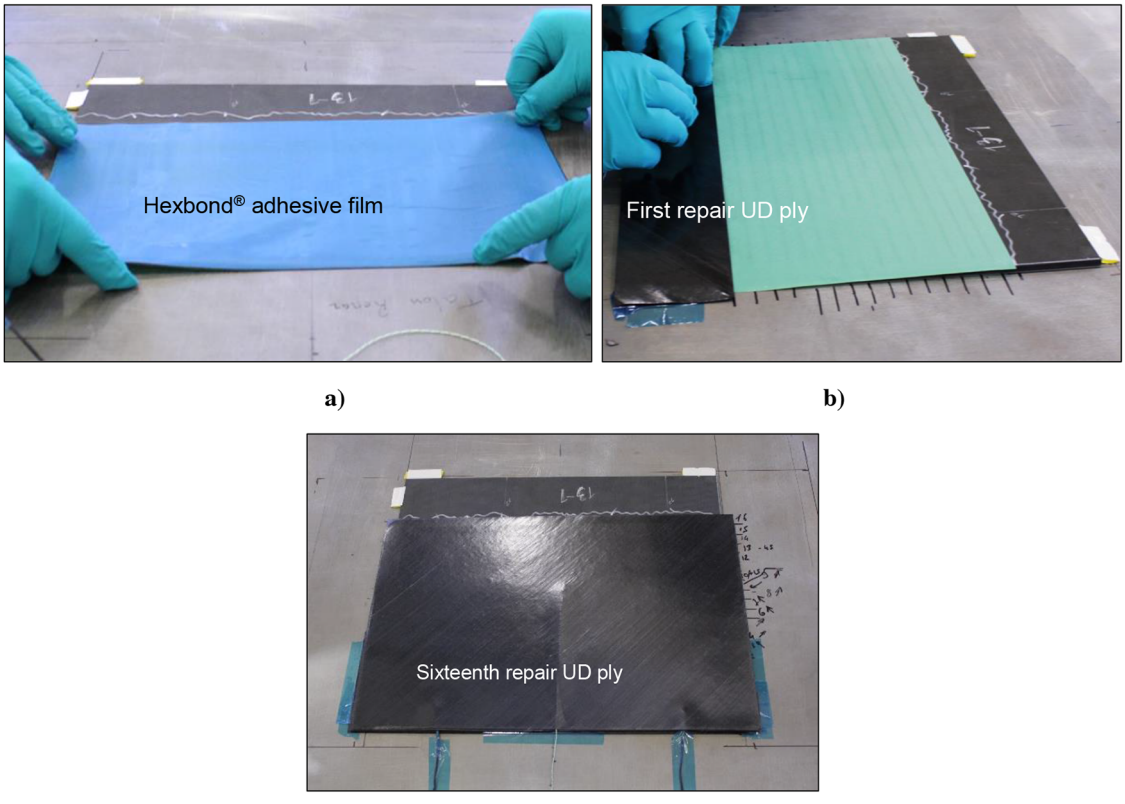

Fig. 10. Repair patch installation with (a) lay-up of the Hexbond® adhesive film with its protective plastic film, (b) placement of the first repair ply and (c) after the placement of the sixteenth repair ply.

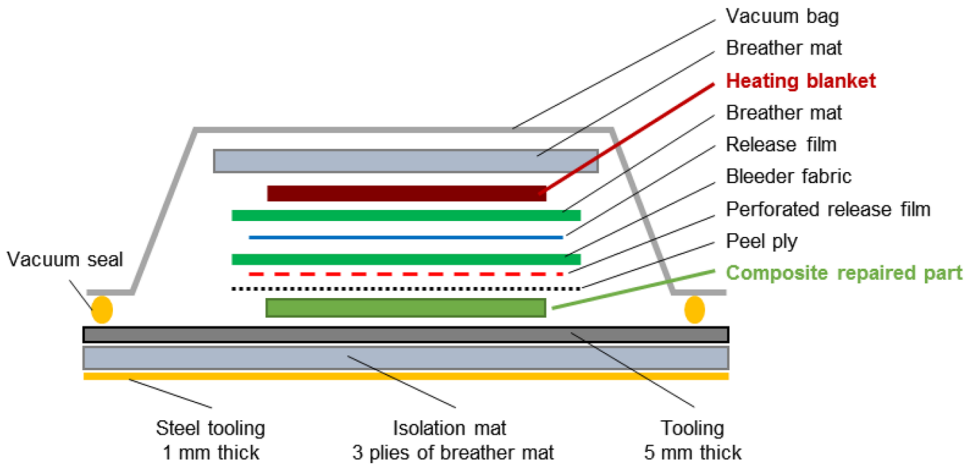

Fig. 11. Scheme of the vacuum bag products (not to scale) for the composite patch curing by heating blanket (according to SRM A350 chapter 51.77.11, see [6]).

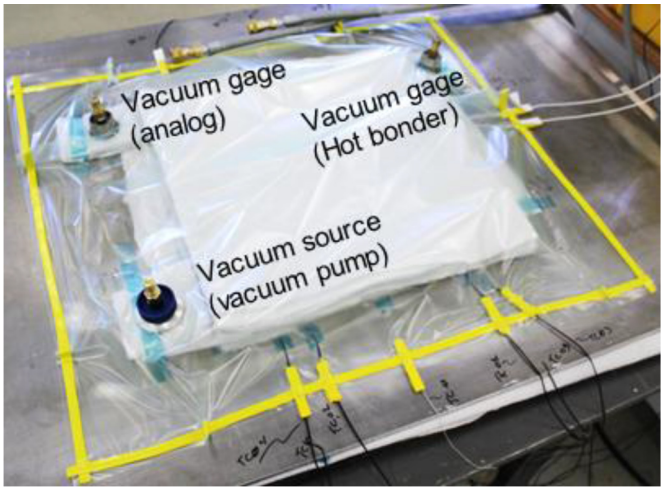

Fig. 12. Overview of the vacuum bag products and the connections to the different thermocouples.

Fig. 13. Portable hot bonder Aeroform AHB-380 (right) and the portable vacuum pomp (left).

The temperature cycle is programed into the hot bonder (cf. Fig. 13). The M21 resin cures at 180 °C for 2 h. An intermediate dwell at 100 °C for 30 min is used in order to homogenise the temperature in the unconsolidated patch prepreg and to promote the movement of resin and removal of entrapped air causing porosities in the material. The temperature ramps are set at 3 °C min^{-1}. The vacuum is applied with an external portable vacuum pump (cf. Fig. 13).

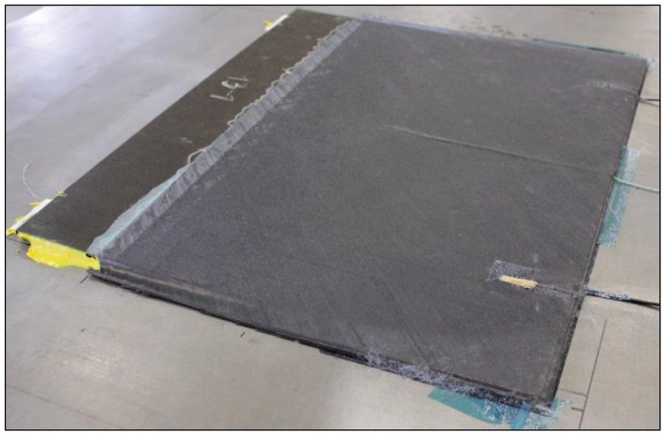

Fig. 14. View of finished repair on "Plate 13" after curing (overlap length of 13 mm).

When the curing cycle is complete, the part is demoulded. The resulting part is shown in Figure 14. Finally, coupons for tensile test are cut from the repaired parent plate using an abrasive water jet machine. The central zone is only considered to eliminate defects in the boundary of the parent plate.

4 Light finite element models and mechanical tests

A light finite element (FE) modelling strategy is used [5,7]. This strategy uses shell elements for the composite laminate and volume elements for the adhesive joint (cf. Fig. 15). The mesh of the composite parent zone is modelled with shell elements of 0.44×0.44 mm dimensions. One volume element of 0.1 mm thick with the same width and length as the composite shell elements is employed to model the adhesive film with a thickness to length ratio of 1:4.

To ensure a continuous transfer of stresses and nodal displacements, each segment of the step repair is linked to the previous one using rigid beam elements. In our applications, there was no adhesive rupture but only a cohesive one, if any. Thus, since we are not interested in studying the interface failure of the adhesive joint (no adhesive rupture) and with the need to have a light FE model, cohesive elements are not considered. This light modelling strategy allows the reduction in computation time and facilitates the experiment/calculation comparisons. The initial implementation of this methodology was programmed in Samcef^{TM} code [5,7] and it was successfully applied in the Abaqus^{TM} code. Details of the number of elements and the degrees of freedom for each of the 6, 8 and 13 mm overlapping length models are given in Table 1.

The shape of the tensile repaired coupon is shown in Figure 16. The repaired coupon is 22 mm wide in the gauge zone, corresponding to the overlap zone. Its end tabs are 30 mm wide in order to avoid a possible material failure at the machine clamps. The zone of 20 mm length approximately located between the overlap and the tab is considered as representative of a non-repaired area. This zone corresponding to the non-repaired zone of the parent zone has the original parent plate of 16 plies, while the reconstituted material in the patch area has one extra ply (repair ply #0) with the same orientation as the repair ply #1. This filler ply is only used to ensure continuity of the bottom surface of the repair, and to provide support for the stacked plies, otherwise there would be ply waviness in the rest of the stack. Thus, this zone has a stacking sequence with 17 plies in total in accordance with composite repair implementation (cf. Fig. 17). As in Figures 2 and 17 uses white arrows to show the loading flow transfer principle from the parent plies to the repair plies.

In this study, we are not concerned by the ultimate tensile strength of the coupon, according to the aeronautical specifications of work for which no damage is allowed (no defect event in general). The behaviour of the ±45° tensile test is matrix dominated, and having the fibres oriented at an angle different from the loading direction, the resulting axial stress − strain curve begins nonlinear because of many reasons which have not been investigated in this study, such as damage initiation in the matrix. We are interested to study the performance of the repair while the 16-ply monolithic non-repaired zone of the material is within its linear regime just before the nonlinear regime. The material behaviour of the FE models is considered as linear elastic without considering non-linearity. This is an arbitrary choice in order to apply the convenient Tsai-Hill (TH) criterion.

In the input material data, the priority characteristics to be identified from the initial parent part are those most influenced by the matrix behaviour i.e. the transverse

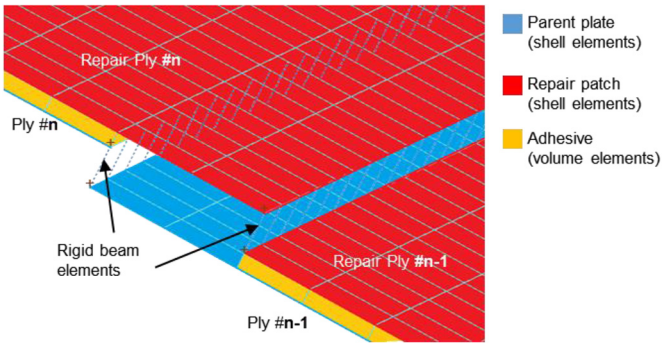

Fig. 15. Mesh detail between two consecutive steps (ply #n and #n-1).

Table 1. Definition of the three meshes per overlap length value.

Step size (mm)	6	8	13
Number of Finite Elements	48 000	58 000	86 000
DoF (Abaqus^{TM} variables)	309 000	367 000	542 000

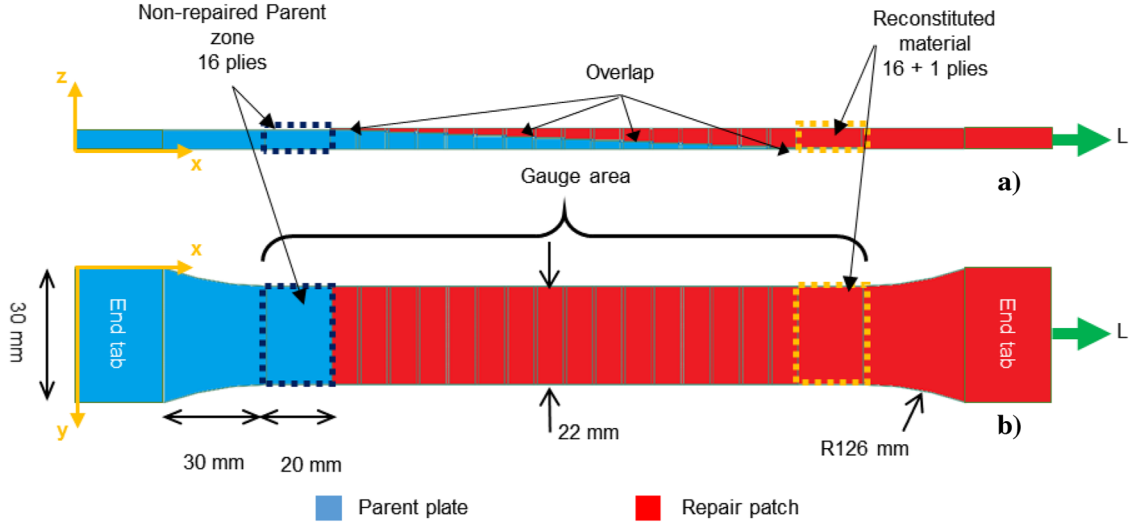

Fig. 16. 3D representation of the FE model (shell thicknesses rendered at their given values) with (a) side view (XZ plane) and (b) top view (XY plane).

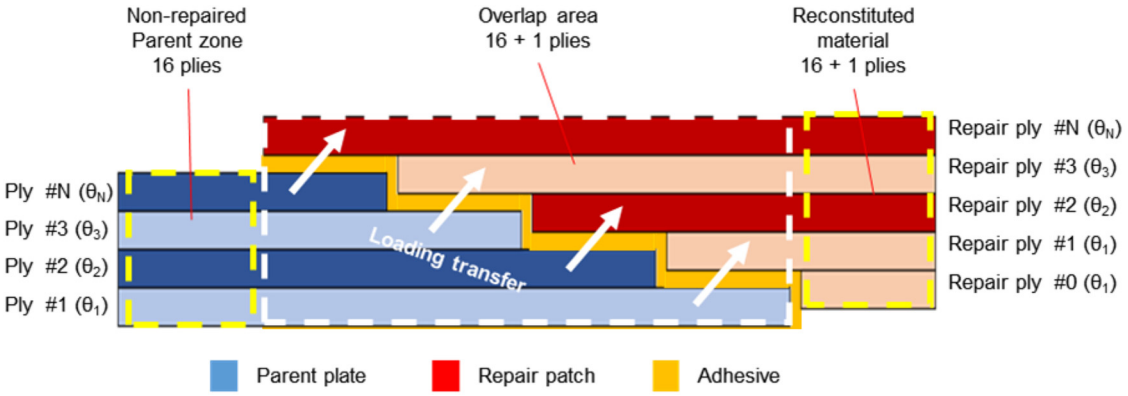

Fig. 17. Scheme of composite repair overlap considerations (not to scale).

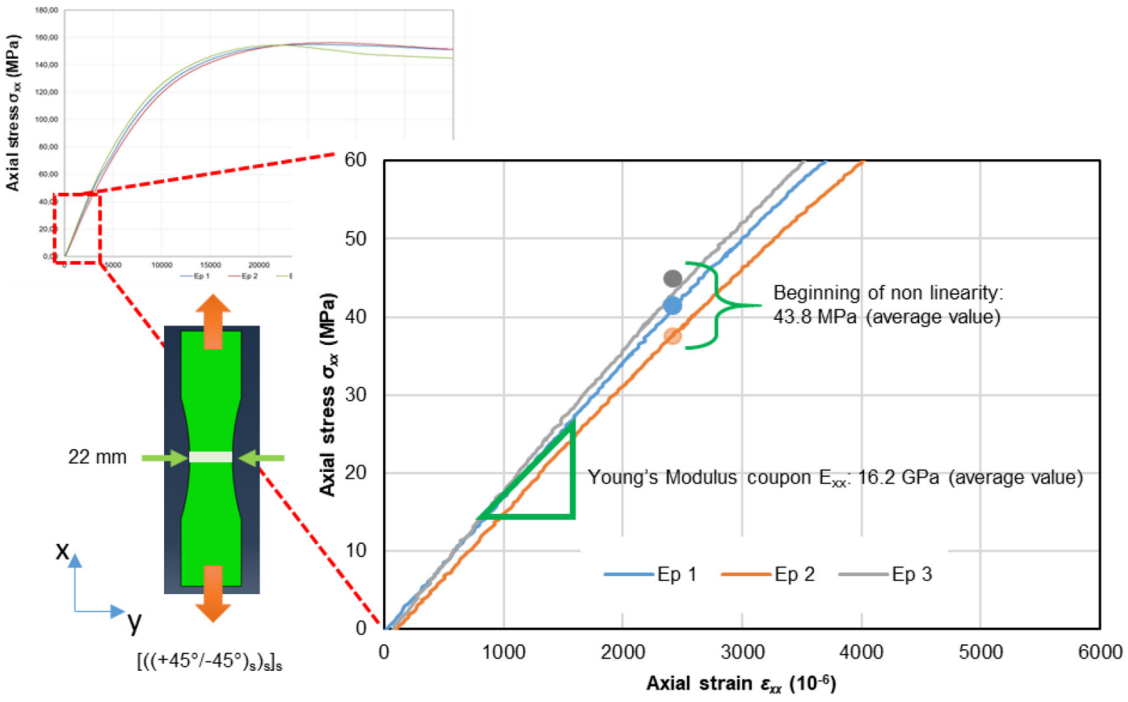

Fig. 18. Inverse identification of the material properties (at the beginning of the non-linear behaviour) using a tensile test on unrepaired specimens extracted from the manufactured mother plate.

Young's moduli $E_2 = E_3$ and the axial-transverse shear moduli $G_{12} = G_{13}$ of the UD prepreg. We have identified these two input material values. Indeed, there are some adjustments to be done compared to the values given by the manufacturer due to the real state of the matrix (ageing ...), the manufacturing conditions and the test configuration. This is achieved through an inverse method by a loop of optimisation reducing the gap by adjustments between numerical and experimental results in tension. For that, specimens are extracted from a non-repaired zone of the 16 plies ±45° plates. These testing coupons, noted "Ep 1", "Ep 2" and "Ep 3", are shaped in the form of a dumbbell (with wider end tabs and a narrow gauge area) in order to control the place where the testing coupon is expected to reach a non-linear response (i.e. away from the clamps of the test machine). The beginning of the nonlinear part of the axial stress-strain curve (cf. Fig. 18) is used in the inverse analysis leading to the elastic and our arbitrary or chosen limit values of shear strength and transverse strength matrix identifications (in red on Tabs. 2 and 3). For the other mechanical properties, the values given by the maker are considered to be reliable (in black on Tabs. 2 and 3).

The material properties of the Hexply® M21/35%/268/T700GC and the Hexbond® adhesive film are indicated in Table 2. The strength values used to calculate the Tsai-Hill (TH) criterion are indicated in Table 3. These values are entered into the FE model to compute the Tsai-Hill criterion for the composite material as a high probability of the issue occurrence. As mentioned before, this test is mainly dominated by the shear and tensile matrix properties, and it is well below the maximum load capacity of the fibres. The values for the tensile strength of

Table 2. Material properties of the Hexply® M21/35%/268/T700GC (in red, the updated properties by inverse identification along reinforcement orientation) and the Hexbond® adhesive film.

UD Ply: Hexply® M21/35%/268/T700GC		Adhesive film: Hexbond®	
Property	Value	Property	Value
Axial Young's modulus E_1 (MPa)	140 500	Adhesive Young's modulus E_a (MPa)	3 800
Transverse Young's modulus E_2, E_3 (MPa)	10 100	Adhesive Poisson's ratio ν_a	0.300
Axial-transverse Poisson's ratio ν_{12}, ν_{13}	0.334	Mean adhesive thickness t_a (mm)	0.100
Transverse-transverse Poisson's ratio ν_{23}	0.171		
Axial-transverse shear modulus G_{12}, G_{13} (MPa)	4600		
Transverse-transverse shear modulus G_{23} (MPa)	3600		
Mean ply thickness t_{ply} (mm)	0.260		

Table 3. Strength of the polymerised ply (in red the limit values obtained by inverse identification along the reinforcement orientation) of the Hexply® M21/35%/268/T700GC and the Hexbond® adhesive film.

Property	Value	Property	Value	Property	Value
Axial tensile strength X_T (MPa)	2 800	Transverse tensile strength Y_T (MPa)	20	Shear strength S (MPa)	23
Axial compressive strength X_C (MPa)	−1 700	Transverse compressive strength Y_C (MPa)	−300		
Average adhesive shear strength in the overlap (MPa)	35	Adhesive tensile strength (MPa)	70	Adhesive peel strength (MPa)	20

the matrix (YT) and the shear strength (S) are below the typical epoxy values, as these values were identified to determine the limit values on the ±45° test configuration. A Mixed Failure criterion developed by [7] is used for the adhesive film. This criterion is based on the work of [11] and [12]. The input data are presented in Table 2.

Three different models are considered, one for each of the overlap lengths respectively, 6 mm, 8 mm and 13 mm.

5 Test calculation comparisons

Three coupons per overlap length were tested in a universal test machine. Here we illustrate with results concerning the 13 mm overlap repair length for the three specimens noted "Ep 13–1", "Ep 13–2" and "Ep 13–3". The non-repaired zone in the parent area was painted for digital image correlation in order to have the stress-strain curve of this particular area (cf. Fig. 19). The zone, with the thinnest cross section because of 16 plies instead of 17 plies in the overlap and the reconstituted zone of the repair patch (cf. Fig. 17), is the zone expected to reach limit values before the others and especially before the adhesive joint repair patch.

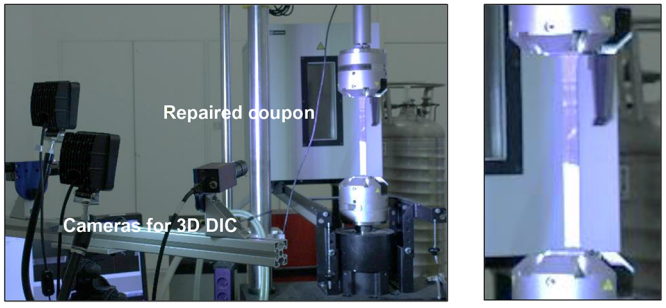

Fig. 19. Axial tensile test configuration with, (a) set-up with two cameras for 3D DIC and (b) zoom of the repaired coupon with its DIC speckle (in white).

The aim is to illustrate that the maximum loading flow (here the shear flow), when it is not applied in the reinforcement orientation, does not depend on the overlap length. This hypothesis will be used to reduce the repair patch extension [2]. According to [2] along the fibre direction, the overlapping length depends on the chosen step ratio. In the other directions, this ratio can be reduced

Table 4. Results of the reference test coupons Ep 1, 2 and 3.

Properties	Coupons (without repair area)			Mean	Std. deviation
	Ep 1	Ep 2	Ep 3		
Axial Young's modulus E_{xx} (GPa)	16.3	15.5	16.9	16.2	0.70
Axial strain ε_{xx} (1E−6)	2 765	2 536	2 760	2 687	131
Axial stress σ_{xx} (MPa)	45.0	39.4	46.9	43.8	3.88
Load L (kN)	4.18	3.67	4.46	4.10	0.40

Table 5. Results of the test coupons Ep 13–1, 13–2 and 13–3.

Properties	Coupons (with repair area)			Mean	Std. deviation
	Ep 13-1	Ep 13-2	Ep 13-3		
Axial Young's modulus E_{xx} (GPa)	15.5	17.0	16.0	16.2	0.77
Axial strain ε_{xx} (1E−6)	2 625	2 844	2 823	2748	130
Axial stress σ_{xx} (MPa)	40.5	48.5	44.7	44.6	4.00
Load L (kN)	3.56	4.28	3.94	3.93	0.36

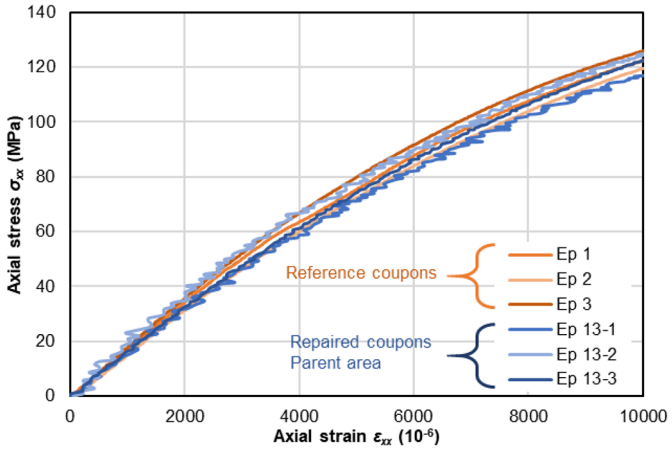

Fig. 20. Axial stress σ_{xx} – strain ε_{xx} curve of the parent area of repair coupons Ep 13-1, 13-2 and 13-3 and reference test coupons Ep 1, 2 and 3.

down to zero. Comparing the test between the repaired composite specimens and the reference coupons, we cannot see any distinction in the mechanical behaviour (cf. Fig. 20). At this moment of the test, the adhesive has not reached a limit value.

Tables 4 and 5 summarize the experimental results for the reference, non-repaired coupons, and the repaired coupons for the non-repaired parent area. We observe that the values for the Young's modulus, as well as the limit values are within the same order of magnitude.

As expected, the place where the limit values are reached is at the parent zone (with cross section reduction compared to the rest of the specimen) between the end tab and the overlap areas. It corresponds to the same situation in the reference coupons. The three overlap ratios exhibit numerically the same behaviour (cf. Fig. 21).

As volume elements are used for the adhesive, they provide information on the out of plane and transverse lap shear. Figure 22 shows the distribution of the shear stresses τ_{xz} at the bondline of each of the 16 steps for the three overlap ratios of 20, 30 and 50. We observe that the stress distribution is maximum at the extremities and minimum in the central steps but below the limit shear value (roughly 13 MPa), and, because of the test configuration, the peel stress values are negligible (less than 1 MPa which represents 1/20th of the limit value, cf. Tab. 3). The stress values have the same order of magnitude for the three overlap ratios [13]. The shear stress shown on Figure 22 is in accordance with typical results in the literature [14], and is not uniform along the bond-line. At both ends of the overlap, we have a peak of shear stresses while at the midpoint of the bond-line the shear stress values are close to zero. For this reason, assessing the adhesive performance with the maximum shear stress is not useful.

According to [7,11,12], a criterion to determine whether the bond has cohesively failed by shear stress is to obtain the area under the curve, which is the total stress per unit length that the adhesive carries (cf. Fig. 23). For epoxy adhesives, the shear strength, i.e. the maximum stress that can be applied into the adhesive along the overlap, is 35 MPa. Here, numerically the maximum shear stress was 13.5 MPa, which is indeed 2.5 times lower than the maximum shear stress for the adhesive. It was observed experimentally that no testing coupon had a failure of the adhesive.

The FE results show that, at a load corresponding to the limit values in the parent composite (TH = 1, cf. Fig. 21), the maximum shear value, calculated in the adhesive (area under the τ_{xz} curve), is 13.5 MPa in both step #1 and step #16. The rest of the steps in between have a less significant value (cf. Fig. 24). All overlap lengths

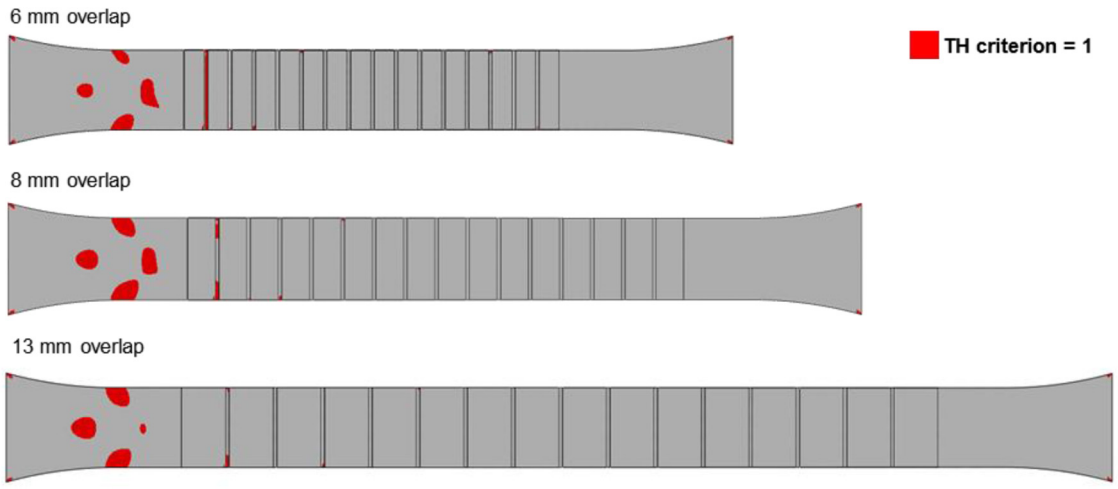

Fig. 21. Tsai-Hill criterion (TH = 1 in red when the chosen limit values are reached) in the FE models for the 6, 8 and 13 mm overlap lengths (from top to bottom).

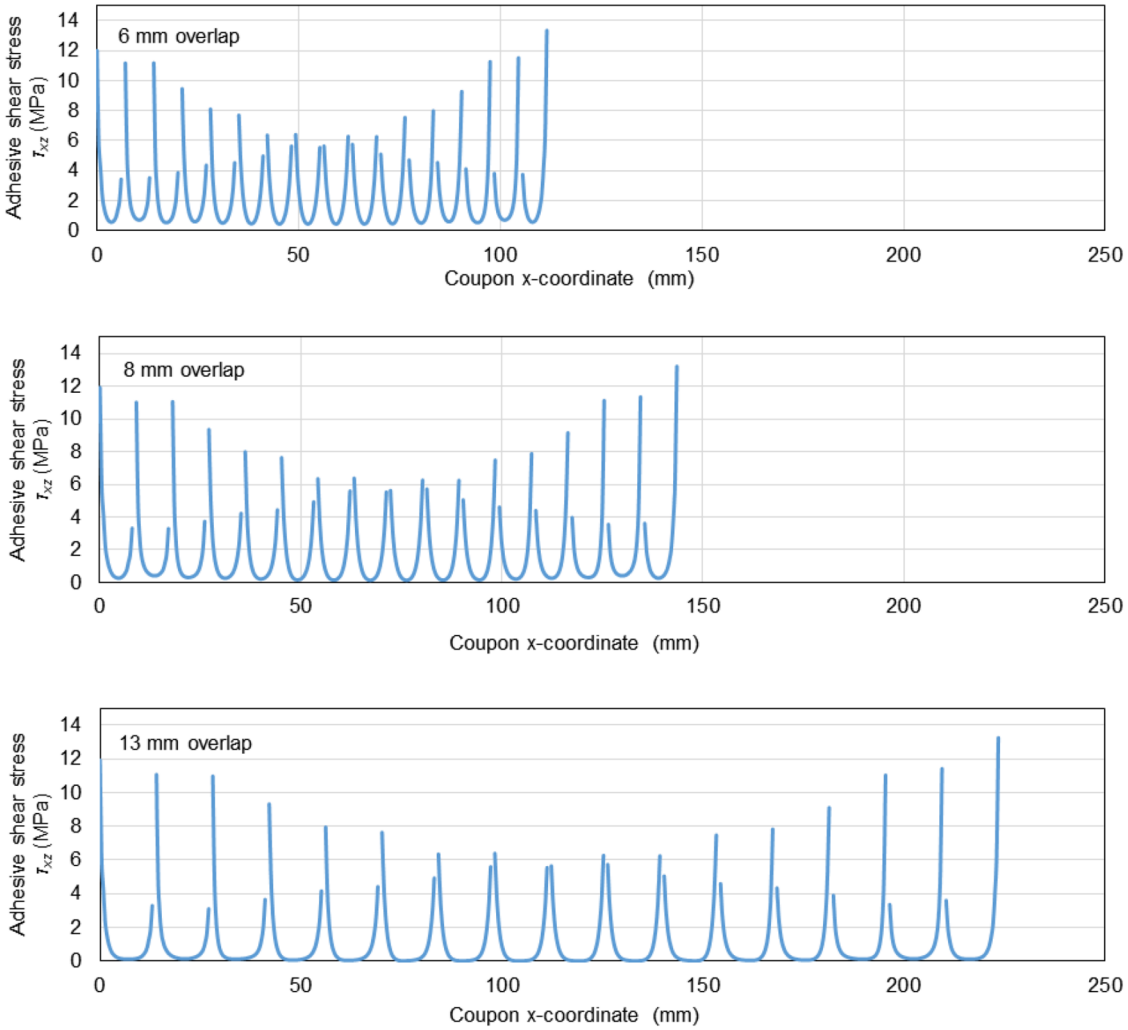

Fig. 22. Shear stress τ_{xz} distribution in the adhesive in each step (from top to bottom) for the 6, 8 and 13 mm overlap lengths.

Table 6. Results of the FE models when the Tsai-Hill criterion is satisfied (TH = 1 for chosen limit values).

Overlap length (mm)	6	8	13
Load L (N)	3 980	3 980	3 980
Displacement u_x of the mobile clamp (mm)	0.52	0.60	0.80
Max area under the curve of τ_{xz} (MPa)	13.63	13.66	14.01
Max axial strain ε_{xx} in the non-repaired parent area (10^{-6})	2 728	2 722	2 764

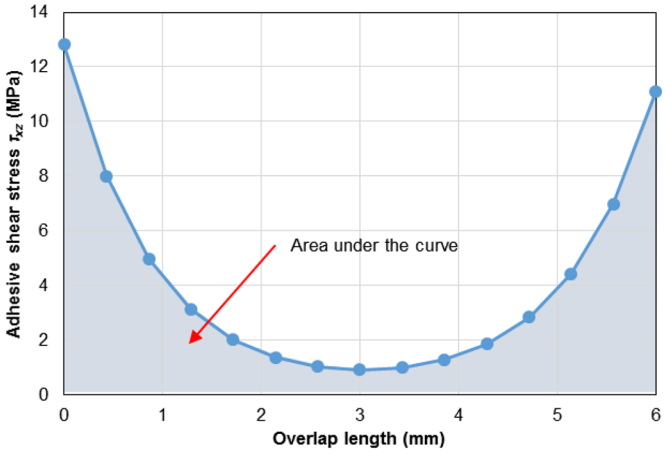

Fig. 23. Determination of the average shear value along the adhesive joint for 6 mm overlap length [7].

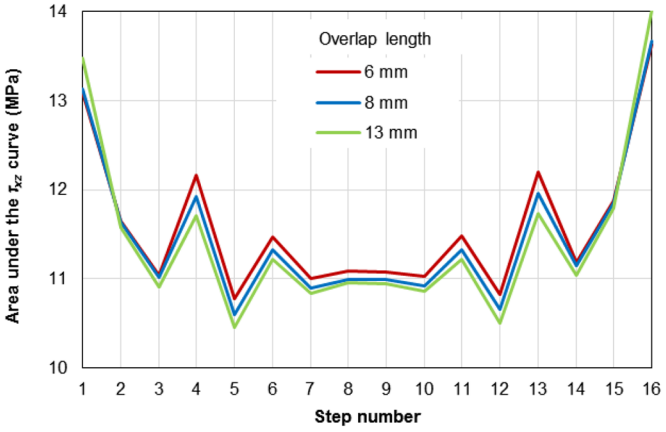

Fig. 24. Area under the curve τxz-step length at each step and for the 6, 8 and 13 mm overlap lengths.

(6, 8 and 13 mm) exhibit average shear lap stresses of the same order of magnitude.

Finally, Table 6 summarizes the data obtained by the FE models highlighting that the three respectively, 20, 30 and 50, overlap ratios (corresponding to 6, 8 and 13 mm overlap lengths respectively) yield the same orders of magnitude for the maximum axial strain ε_{xx} in the non-repaired parent area (i.e. in the monolithic parent zone). This suggests that reduction of the overlap length is beneficial [2].

6 Conclusions

In this paper, the different stages of a repair process on an aeronautical composite material have been presented.

First, the machining tool generates an abrasive waterjet with specific parameters adapted to composite blind machining [10]. A control system captures and analyses images to generate a mapping of the machining work to take into account the ply thickness variability allowing both adaptation of the depths to the ply thickness variability between each machining step [9], and archiving of the result when the repair machining work is complete.

Second, the repair procedure is followed using the industrial set-up with a hot bonder. The studied plate of 16 plies of UD Hexply® M21/35%/268/T700GC prepreg with an unusual stacking sequence $[+45/-45/-45/+45/+45/-45/-45/+45]_s$ was repaired for 3 overlap lengths (6, 8 and 13 mm) according to the aeronautical requirements.

Third, for the different overlapping lengths, a comparison was made between computations and physical tests on specimens taken from the repaired plate and subjected to an axial load. The mechanical tests showed that the stepped lap of the repaired zones are not the weak link of the specimens, whatever the overlap lengths.

Fourth, an innovative multi-scale model is employed in which only the adhesive zone consists of volume finite elements. The FE results show that at a load corresponding to the chosen limit values in the parent composite, the maximum shear value calculated in the adhesive is below the limit shear value, whatever the steps and the overlap lengths.

This illustrates that the joint patent [2] held by the Clement Ader Institute, the SME Composites Expertise & Solutions and the SME Bayab Industries operates. The simple idea of [2] indicates that a nominal overlap length is only necessary if the loading is strictly in the direction of the UD ply fibres. Taking profit from the joint patent, the repair approach should reduce the patch size as compared to the conventional approaches by 70% [1]. Finally we note that a French repair workshop exists since 2010 in the GDR (Research Group) 3371 MIC "Mise en œuvre des composites et propriétés induites" (Composite

Manufacturing and Induced Properties), showing the relevance of the French composite repair activity. The composite repair activities are carried out in particular at Clement Ader Institute (France) in cooperation with the SME Composites Expertise & Solutions (France), for more than 20 years, and recently, since 2019, with the Airbus Customer Services for performing repair tests at high altitude at Pic du Midi (2877 m) in the Pyrenees Mountains (France).

The authors want to declare their gratitude for their helpful advice to Sebastien Dupouy [6], A350 Industrial Manager of Aircraft Repairs & Retrofits, and Guillaume Ferrer [6], Embodiment Industrialization Manager, in charge of A350 composite repair process development and the Repair LAB in Airbus Customer Services (France). The authors acknowledge CONACyT of Mexico for the PhD scholarships provided to Sergio Albano Avila Hernandez and Alexander Morales Gomez (Mexico). We would like to thank Olivier Cherrier and Marc Chartrou from Clément Ader Institute (France) for their valuable technical contribution to the mechanical tests and Thomas Beaucourt, technician in Bayab Industries (France) for the machining of the composite plates. Finally, we would like to thank the French organizing team of the 24th edition of CFM conference, Congrès Français de Mécanique held in Brest (France) in 2019, for its invitation for a keynote lecture on the composite repair topic, thus contributing to promote our scientific efforts in this field of both industrial and scientific challenges.

References

[1] ca 2769668, Method for repairing a wall consisting of a plurality of layers, filling date: 28-07-2010, publication date: 17- 02–2011. Owners: Jedo Technologies then Bayab Industries (France), Composites Expertise & Solutions (C.E.S.) (France), Institut Clément Ader – Université Paul Sabatier (France), http://bases-brevets.inpi.fr/en/document-en/FR2949092.htm, 2010.

[2] F. Collombet, Y.H. Grunevald, L. Crouzeix, B. Douchin, R. Zitoune, Y. Davila, A. Cerisier, R. Thevenin, *Repairing composites, in book Advances in Composites Manufacturing and Process Design* (Elsevier Ltd., 2015), Chap. 10, pp. 197–227

[3] Bonded Repair Size Limits, EASA CM No.: CM-S-005 Issue 01 issued 11 September 2015

[4] A. Baker, J. Wang, Proposed through-life management approaches for adhesively bonded repair of primary structures, Int. J. Adhes. Adhes. **87**, 151–163 (2018)

[5] F. Collombet, L. Crouzeix, Y.-H. Grunevald, Y. Davila, B. Douchin, N. Rocher, Réparation de pièces structurales monolithiques aéronautiques. Comptes Rendus des JNC 21, 21ème Journées Nationales sur les Composites, Bordeaux (France), 1–3 juillet 2019, https://hal.archives-ouvertes.fr/hal-02423014/ (in French)

[6] S. Hanser, G. Ferrer, S. Dupouy, A350 XWB composite bonded repair, New technology for new aircraft, Fast#61, 2018, pp. 11–18

[7] A. Cerisier, Prediction of the behavior of a primary step-lap bonded repair : application of a methodology with technical evaluators, Ecole doctorale MEGeP, Institut Clément Ader (ICA-Toulouse), Toulouse III PhD thesis (in French), 2017

[8] H. Bendemraa, P. Compston, Ph.J. Crothers, Optimisation study of tapered scarf and stepped-lap joints in composite repair patches, Compos. Struct. **130**, 1–8 (2015)

[9] Y. Davila, L. Crouzeix, B. Douchin, F. Collombet, Y.-H. Grunevald, Spatial evolution of the thickness variations over a CFRP laminated structure, Appl. Compos. Mater. **24**, 1201–1215 (2017)

[10] F. Cénac, F. Collombet, M. Déléris, R. Zitoune,Abrasive water jet machining of composites, in J. Paulo Davim (Ed.), Machining Composite Materials, ISTE Ltd (2010) Chapter 4pp. 167–180

[11] J.M. Whitney, R.J. Nuismer, Stress fracture criteria for laminated composites containing stress concentrations, J. Compos. Mater. **18**, 263–265 (1974)

[12] J.Y. Cognard, L. Sohier, P. Davies, A modified Arcan test to analyze the behavior of composites and their assemblies under out-of-plane loadings, Compos. A **42**, 111–121 (2011)

[13] P. Davies, L. Sohier, J.Y. Cognard, A. Bourmaud, D. Choqueuse et al., Influence of adhesive bond line thickness on joint strength, Int. J. Adhesion Adhes. **29**, 724–736 (2009)

[14] L. Sohier, J.Y. Cognard, P. Davies, Analysis of the mechanical behaviour of adhesively bonded assemblies of composites under tensile-shear out-of-plane loads, Compos. A **53**, 65–74 (2013)

Cite this article as: F. Collombet, Y. Davila, S. Avila, A. Morales, L. Crouzeix, Y.-H. Grunevald, H. Hernandez, N. Rocher, F. Cénac, Proof of a composite repair concept for aeronautical structures: a simplified method, Mechanics & Industry **20**, 812 (2019)